IEEE Access
Multidisciplinary | Rapid Review | Open Access Journal

Received 17 September 2023, accepted 6 October 2023, date of publication 10 October 2023, date of current version 18 October 2023.

Digital Object Identifier 10.1109/ACCESS.2023.3323405

RESEARCH ARTICLE

A Route Planning and Traffic Control Model for Autonomous Intersections by Minimizing Conflict Zones

YANG LIU[1], KEJUN LONG[1], AND WEI WU[2]

[1]Hunan Key Laboratory of Smart Roadway and Cooperative Vehicle-Infrastructure Systems, Changsha University of Science and Technology, Changsha, Hunan 410114, China

[2]College of Traffic and Transportation, Chongqing Jiaotong University, Chongqing 400074, China

Corresponding author: Wei Wu (weiwu@cqjtu.edu.cn)

This work was supported in part by the National Natural Science Foundation of China under Grant 52172313, in part by the Changsha Science and Technology Plan Project under Grant kq2107009, in part by the Hunan Provincial Natural Science Foundation of China under Grant 2023JJ30033, in part by the Hunan Provincial Innovation Foundation for Postgraduate under Grant CX20210744, and in part by the Changsha City Science and Technology Major Special Project under Grant kh2301004.

ABSTRACT Most existing studies on autonomous intersection management (AIM) primarily focus on modeling and resolving conflicts between vehicles within an intersection, assuming predetermined routes of the autonomous vehicles (AVs) as exogenous inputs. Additionally, these studies presume scenarios in which AVs traverse the intersection at a constant speed without stopping. However, such scenarios are difficult to realize under heavy traffic demand. To address this issue, this study first discretized the intersection into numerous grids and proposed formulations to calculate the time at which the vehicles enter and exit a given grid at different speeds and accelerations based on the outer-boundary-projection dimension-reduction method. Thereafter, a bi-level programming model was established to optimize the route choices and traffic control schemes. The upper-level model aimed to minimize the conflicts within the intersection zones, considering the lane options for vehicles entering and exiting the intersection as the decision variable to optimize the AV routes. In addition, the lower-level model strived to minimize the delay for all upcoming vehicles. The time when a vehicle enters an intersection and whether it stops are utilized as decision variables. Based on the sliding time-window technique, the proposed model was transformed into a mixed-integer linear programming (MILP) problem, which is compiled by a mathematical programming language (AMPL) and solved by CPLEX. The numerical analysis shows that the proposed models significantly reduced the conflicts between the vehicles, and consequently, improved the space utilization of the intersection, reduced vehicle delays, and saved a significant amount of energy.

INDEX TERMS Autonomous intersection management (AIM), route planning, all-direction lanes, mixed-integer linear programming (MILP), intersection.

I. INTRODUCTION

Intersections are widely recognized as bottlenecks of traffic flow in urban road networks [1]. In recent years, many studies have focused on traffic control at intersections, with the majority of these studies aimed at optimizing traffic signals timing scheme to improve traffic efficiency at intersections [2]. Although intersection signal control has made significant progress in improving the safety and throughput of traffic flows, it still presents notable disadvantages that cannot be overlooked, they are listed as follows:

i. The unpredictable and fluctuating traffic arrivals from multiple directions at intersections can lead to suboptimal lane and phase configurations, resulting in reduced vehicle mobility during green lights [3], [4].
ii. The duration of the time interval between two sequential green light phases at an intersection is affected by factors such as clearance distance, clearance speed,

The associate editor coordinating the review of this manuscript and approving it for publication was Emanuele Crisostomi.

entering speed, and passing time of vehicles. However, the transition between phases often results in wasted space and time resources at the intersection [5].

Consequently, numerous researchers and urban planners have sought to enhance the traffic control methods at intersections. Recently, the advancement of autonomous driving technology has presented new challenges to traffic control, while also providing opportunities for addressing the aforementioned problems [6], [7].

As far as the authors know, Dresner and Stone first proposed the concept of autonomous intersection management (AIM), which involves the use of autonomous vehicles (AVs) that cooperate to cross intersections without the need for signal control [8], [9]. Previous studies have demonstrated that AIM can effectively address the two signal control issues mentioned earlier, thereby enhancing traffic efficiency [10], [11]. AIM can be classified into two categories, i.e., centralized and distributed. Centralized control relies on vehicle-to-infrastructure (V2I) communication and utilizes infrastructure/intersection managers for traffic control. In this mode, a central controller makes global decisions regarding the right-of-way for all AVs [12].

Numerous studies have focused on centralized control strategies to improve traffic efficiency at intersections while prioritizing traffic safety. These studies aim to optimize the order and timing of vehicle entry into intersections [13], [14]. For instance, in [15] proposes a cooperative scheduling mechanism for autonomous vehicles passing through an intersection without traffic lights. The mechanism uses priority setting, window searching and trajectory planning to ensure safety and efficiency. In [16], proposes a robust autonomous intersection control (AIC) approach with global optimization scheduling and demonstrates its superiority in transportation efficiency and robustness. In [17], devised a collaborative, sequence-based control system and put forward two control strategies to determine the safe passing sequence of vehicles at intersections. The efficiency of the proposed system was confirmed via the use of microscopic simulations. In [18], created a dynamic programming model aimed at maximizing intersection throughput at signal-free intersections. In order to mitigate traffic conflicts, they proposed a stochastic look-ahead technique based on the Monte Carlo tree search algorithm. Reference [19] proposed a priority-based, signal-free control algorithm and a discrete forward-rolling optimal control algorithm. To minimize energy consumption and maximize traffic capacity, [20] optimized vehicle routes at intersections by establishing a correlation between minimizing energy consumption and maximizing throughput. Reference [21] proposed a two-level optimization model for vehicle scheduling and trajectory optimization, which proved to be more effective than the first-in-first-out (FIFO) method in reducing vehicle delays and fuel consumption.

Distributed control relies on vehicle-to-vehicle (V2V) communication, enabling vehicles to independently develop their optimal intersection passage plans by gathering local traffic information [22]. Specifically, it can be categorized into heuristic-based and optimization-based control [23], [24]. For heuristic control, [25] introduced the concept of safety driving patterns, which utilizes a spanning tree to describe the solution space of allowable movement schedules with safety constraints. Accordingly, they proposed four trajectory planning algorithms and used the spanning tree to determine the driving plans with least execution times. Based on this outcome, [26] proposed a cooperative control strategy that combines Monte Carlo tree search with heuristic rules to efficiently discover a nearly globally optimal passing order for vehicles at intersections. For optimization-based control, [27] modeled the intersection control problem as a distributed computing problem of classical mutual exclusion and designed a solution algorithm accordingly. Reference [28] proposed a decentralized coordination method that combines optimal control with model-based heuristic algorithm. Reference [29] proposed a distributed conflict resolution mechanism to achieve real-time feasible solutions for large-scale combinatorial optimization problems. Furthermore, [30] proposed a fully distributed control method built upon a fully distributed model predictive control approach.

The aforementioned studies have enabled safe and efficient passage of vehicles through intersections without signal control, with reduced traffic delays and improved traffic efficiency of the intersections. In particular, numerous research results have been reported for optimizing vehicle passing order (i.e., the sequences for vehicles entering the intersection) and the entering time. However, most existing studies assume predetermined routes of the AVs and use them as exogenous inputs, and assume that the vehicle travels at a pre-determined speed as prescribed by the model, resulting in the following shortcomings:

i. Most studies have only considered a few conflict points at the intersections [31], [32] and focused on optimizing the order of vehicles entering the intersections to avoid collisions, without considering the optimization of the vehicle routes inside the intersections. However, route optimization can significantly reduce conflicts between vehicles at intersections. For example, [33] constructed a mixed-integer programming model to optimize the vehicle routes within intersections, demonstrating that optimizing the route is an efficient approach to increase traffic efficiency at intersections compared to optimizing entering time. Nonetheless, their research did not consider the optimal utilization of the intersection space, which may diminish the traffic efficiency.
ii. Most AIM studies assume that vehicles pass through intersections at a predetermined speed without stopping, which is difficult to realize in case of heavy traffic flow at intersections. To address this issue, [19] designated speed adjustment zones on the entry lane and set the stop line on the road section, where vehicles can adjust their speed before entering

the intersection. Although this method can resolve the issue of vehicle acceleration inside intersections, it changes the organization of traffic flow in the intersection area, reduces the queuing space of the intersection, and is difficult to replicate in the field.

Thus, this study proposes an approach to resolve the aforementioned limitations and achieve efficient traffic flow at intersections. The contributions of the study are summarized as follows.

1) To minimize the conflict zones, the vehicle routes inside the intersections were optimized before entering the intersections based on "all-direction" lanes, where the entry lanes were not dedicated to certain traffic flows, i.e., an entry lane can accommodate all left turns, through passes, and right turns [34], [35], [36]. Through route planning, the utilization of space resources at intersections was enhanced, and conflicts between vehicles at the intersections were reduced.

2) Contrary to the existing literature, which assumed that vehicles would pass the intersections at a predetermined speed without stopping [19], [26], [31], [34], [37], [38], the present study takes into account the possibility of AVs halt and restart at the intersections during heavy traffic flows. By considering vehicle stoppage as an optimization decision variable, conflicts between AVs at intersections are separated, enabling the optimization of the ideal entry time for each vehicle.

The remainder of this paper is organized as follows. The problem description is presented in Section II, which intuitively expounds the key research points. The model parameters are listed in Section III. The modelling procedure of the proposed model is detailed in Section IV, which includes the model for determining the instant at which the vehicles enter and exit the grids, route optimization model, and conflict separation model. Thereafter, the results of the model solution are discussed in Section V. The model validation and the benefits of the proposed model are summarized in Section VI. Section VII concludes this paper.

II. PROBLEM DESCRIPTION

In this study, we determined the internal routes of vehicles at intersections by considering their entry and exit lanes, as illustrated in Fig. 1. We discretized the intersection into a series of grids and identified the specific grids traversed by each vehicle as it followed its chosen route. By analyzing the intersection in this manner, we were able to accurately determine the routes of vehicles As depicted in Fig. 1a, if the routes taken by vehicles are not optimized, it may lead to overlapping of routes and concentration of conflict zones. To mitigate these concerns, we have developed an optimization approach that optimizes the routes depicted in Fig. 1b. Notably, these optimized routes demonstrate a reduction in overlap. The second challenge addressed in this paper concerns the optimization of vehicle entry times and speed at the intersection, with the aim of minimizing potential conflicts and reducing total delays under diverse operating conditions.

III. PARAMETER DESCRIPTION

The parameters in the model are described in Table 1.

IV. MODEL FORMULATION

The proposed model is primarily composed of three components:

i. Calculation model of the time when vehicles enter and leave grids
ii. Route optimization model of vehicles inside the intersection
iii. Traffic control model

The calculation model computes the time required for vehicles to enter and exit the grid at various speeds, and it is employed to determine the grid set of all routes. In addition, the route optimization model of the vehicles optimizes the vehicle routes inside the intersections according to the entry, turning, and exit lanes, in order to determine the potential conflict grids between the vehicles and minimize the number of vehicles clearing the grid. Finally, the traffic control model separates the potential conflicts by optimizing the time at which the vehicles enter the intersection, considering the route optimization results as inputs and the minimum total delay of the vehicle as the goal.

A. CALCULATION MODEL OF TIME WHEN VEHICLES ENTER AND LEAVE GRIDS

In the optimization of vehicle trajectory at intersections, most previous studies assume that the vehicle passes through the intersection at a constant speed without considering the possibility of stopping and restarting before the vehicle reaches the stop line. Herein, we consider whether the vehicle will stop or not as a variable to establish a calculation model for determining the time at which the vehicles enter and exit the grid, as explained in the following steps:

(1) Discretizing the conflict zones inside the autonomous intersection: First, the internal zone is segmented into small numbered grids and a rectangular coordinate system is established inside the intersection, according to which the boundary equation of each grid is determined.

(2) Determining the grids where all vehicle routes cross the intersection: At the autonomous intersection of the all-direction lanes, the entry and exit lanes of the intersection were numbered. All vehicle routes inside the intersection were determined according to multiple combinations of the entry and exit lanes in each direction. The boundary of each route was determined by considering the physical size of the vehicles, wherein the turning route was modeled based on an elliptic curve and the through route was modeled according to a linear equation. The grid boundary and route boundary equations determined whether the grid is traversed by the route. Here, $\varphi_{g,o_i,d_i,r}$ denotes a binary variable, indicating whether grid g is on route r determined by o_i *and* d_i. In case $\varphi_{g,o_i,d_i,r} = 1$, grid g is on route r; otherwise,

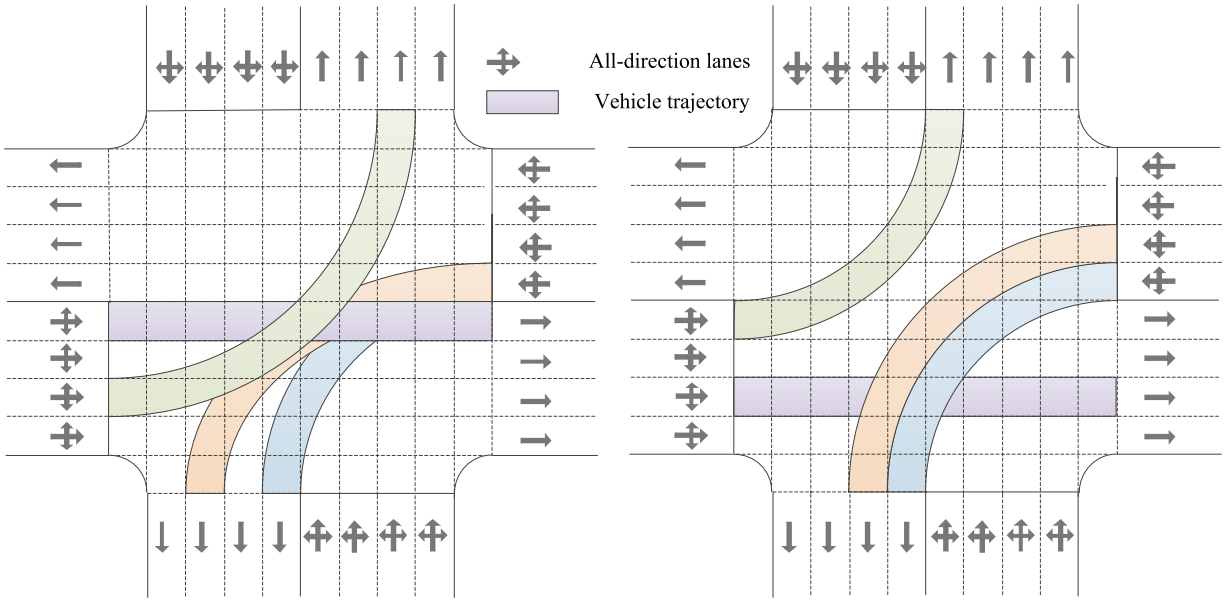

a) Routes taken by vehicles not optimized b) Routes taken by vehicles optimized

FIGURE 1. Problem description.

TABLE 1. Notations and parameters.

Sets	
I	Set of number of vehicles
I_n	Set of vehicles in time window n
R	Set of routes
G	Set of all grids
O, D	Set of approaching directions and exiting directions, respectively
$\{(g,i,j),\ldots\}$	Set of potential conflict of vehicles i and j on grid g, $\forall i,j \in I_n$, $g \in G$
Parameters	
T_i	Theoretical arrival time of vehicle i at intersection (s)
v_c	Speed at which vehicles approach the intersection (m/s)
v_i	Speed at which vehicle i enters the intersection (m/s)
$t_{g,r_i,v}, t'_{g,r_i,v}$	The time when vehicle i enters and exits grid g with velocity v while following path r
M, M_1	A large positive number
Variables	
$\varphi_{g,o_i,d_i,r}$	A binary variable, $\varphi_{g,o_i,d_i,r} = 1$ where grid g is on route r determined by o_i and d_i, otherwise $\varphi_{g,o_i,d_i,r} = 0$
$\Phi_{i,r}$	A binary variable, $\Phi_{i,r} = 1$ where vehicle i passes through the intersection from route r; otherwise $\Phi_{i,r} = 0$
$\rho_{v,i}$	A binary variable, $\rho_{v,i} = 1$ where vehicle i enters the intersection with an initial velocity v, otherwise $\rho_{v,i} = 0$
$\sigma_{i,g}$	A binary variable, $\sigma_{i,g} = 1$ where vehicle i passes through grid g; otherwise $\sigma_{i,g} = 0$
$y_{i,j}$	A binary variable, $y_{i,j} = 1$ where vehicle j enters the same grid before vehicle i; otherwise $y_{i,j} = 0$
l_i', L_i'	The optimal entry and exit lanes vehicle i is selected after route optimization
Ω_g	Number of vehicles clear grid g in all vehicles i
T_i'	The actual arrival time of vehicle i at the intersection
T_i''	The time when vehicle i enters the intersection

$\varphi_{g,o_i,d_i,r} = 0, o \in O$ *and* $d \in D$, wherein O and D indicate the approaching and exiting direction sets, respectively; o_i indicates the approaching direction of vehicle i, where $i \in I, o \in O$, and d_i is the exit direction of vehicle i; g is a grid, where $g \in G$, and G denotes the set of all grids.

(3) Calculating the time required by vehicles to occupy the grid when passing through the intersection: First, the location points of the vehicles entering and exiting the grid should be calculated, and thereafter, the duration for which the grid is occupied by the vehicles is calculated. The location points of the vehicles entering and exiting the grid may correspond to the intersection points of the grid and route boundaries or the grid vertex. Taking point A of the vehicle entering the grid and point B of the vehicle leaving the grid as an example (As

shown in Fig. 2), the time and speed of the vehicle running from point A to point B are calculated. Upon entering the intersection, it is strictly forbidden for vehicles to come to a halt within the confines of the internal intersection area. It is noted that there are four scenarios of vehicle speeds when traveling from point A to B (As shown in Fig. 3). The algorithm to determine travel speed is presented in Table 2.

In the algorithm presented in Table 2, the first step involves determining the intersections between vehicle trajectory boundaries and grid lines. To explain this process, consider Fig. 2 as an illustrative example. Fig. 2 illustrates the path of a left-turning vehicle within the intersection. The points of intersection between the inner trajectory boundary and grid lines are depicted in green, while those between the outer boundary and grid lines are designated in blue. Furthermore, the vertices of the grids within the trajectory's spatial domain are denoted by orange points. The black points are the projected points of the blue points and orange points on the outer boundary trajectory, as indicated by steps 1 to 10 in the algorithm.

Subsequently, step 11 in the algorithm determines the entry and exit points for each grid. For instance, taking the red grid in Fig. 2 as an example, the points where the trajectory enters and exits the grid are denoted as points A and B, respectively. Step 12 calculates the distance between the entry and exit points, denoted as $|AB|$, which depends on whether the vehicle follows a turning path, where $|AB| = \int_{x_{A,g}}^{x_{B,g}} \sqrt{1 + y'(x)^2}dx$, or a straight path, where $|AB| = \sqrt{[(x_{B,g}{}^- x_{A,g})^2 + (y_{B,g}{}^- y_{A,g})^2]}$. By calculating the time and velocity at which the vehicle passes point B, we can determine the time and velocity at which the vehicle exits the red grid.

It is noteworthy that vehicles may need to accelerate within the intersection, so it is required to ascertain if there is acceleration within segment AB. This determination is guided by the velocity-time graph, as illustrated in Fig. 3, which exhibits four possible cases: acceleration followed by constant velocity (as illustrated in cases 3 and 4 in Fig. 3), constant speed motion (as shown in case 1 in Fig. 3), and uniformly accelerated motion (as depicted in case 2 in Fig. 3).

The evaluation of acceleration in segment AB begins by examining whether the vehicle's velocity at point A, denoted as $v_{i,g,A}$, equals to the maximum allowable speed, V_M. If $v_{i,g,A} = V_M$, it indicates that the vehicle travels at a constant speed throughout AB, as displayed in case 1 in Fig. 3. If $v_{i,g,A} < V_M$, traveling at a constant acceleration with an initial velocity of $v_{i,g,A}$ and an acceleration of a until reaching V_M covers a distance of $\frac{V_M^2 - v_{i,g,A}^2}{2 \cdot a}$. This distance is compared with $|AB|$ and $|AB| + d_c$. When $\frac{V_M^2 - v_{i,g,A}^2}{2 \cdot a} \geq |AB| + d_c$, it signifies that the vehicle has not reached the maximum speed by the time it passes point B, and it continues to accelerate throughout AB, as depicted in case 2 in Fig. 3. When $\frac{V_M^2 - v_{i,g,A}^2}{2 \cdot a} < |AB|$, it indicates that the vehicle has already reached its maximum speed

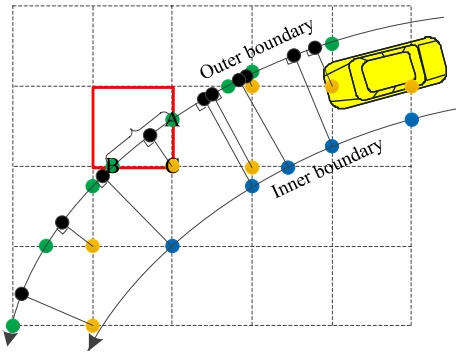

FIGURE 2. The points that a vehicle entering and exiting a grid.

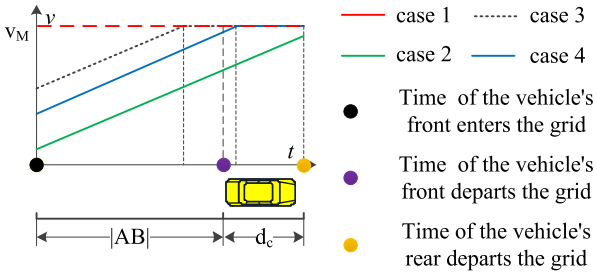

FIGURE 3. V-T of vehicle entering and exiting the grid.

before arriving at point B, as demonstrated in case 3 in Fig. 3. Due to the consideration of the vehicle's length, denoted as d_c, the velocity of the vehicle's front reaching point B and the velocity of its rear leaving point B are different. When $|AB| \leq \frac{V_M^2 - v_{i,g,A}^2}{2 \cdot a} < |AB| + d_c$, it indicates that the vehicle's front end reaches point B without attaining maximum speed, while the rear end achieves the maximum speed upon departing from point B. As illustrated in case 4 in Fig. 3. For the four cases described above, we utilize distinct velocity-displacement formulas to compute the vehicle's time $t_{(i,g,B)}$ and velocity $v_{(i,g,B)}$.

According to the calculation model for the time of vehicles entering and exiting the grid, the time when the vehicle's front enters the intersection and the time at which its tail exits the grid can be calculated at a given speed of the vehicle entering the intersection.

B. ROUTE OPTIMIZATION MODEL AT INTERSECTIONS

The route optimization model for intersections comprises the upper-level model of a bi-level model. The vehicle routes at the intersections were determined using both the entry and exit lanes. As each entry may turn left, right, or travel straight, the vehicles can choose from several route choices available at the intersections. Considering the intersection of an eight-lane bi-directional road as an example (as shown in Fig. 4), there are 16 potential routes for vehicles turning left in the east approaching direction, with the curve representing the centerline of the vehicle's turning route. The grid for each route can be calculated using the method described in Section IV-A. Importantly, the location and size of the conflict zone generated at the intersection will vary

TABLE 2. Algorithm for determining the time at which a vehicle enters and exits grids.

Input vehicle information data, including approaching direction, entry lane, exiting direction, exit lane, and initial speed

For i in I all vehicle sets

If turning vehicles

Determine the internal and external boundary equations of the vehicle routes at the intersection according to the elliptic equation and calculate the range of x- and y-coordinates

Set up the simultaneous equation of route inner boundary equation and grid boundary equation to obtain the intersection point set P_L (As shown by the blue point in Fig. 2)

Set up the simultaneous equation of route outer boundary equation and grid boundary equation to obtain the intersection point set P_R (As shown by the green point in Fig. 2)

Set of grid vertices P_T within the zone in which the inner and outer boundaries of the route are determined (As shown by the orange point in Fig. 2)

For p in $P_{L,T} = P_L \cup P_T$

Calculate the points projected to the outer boundary equation to obtain the projection point set $P_{L',T'}$ (As shown by the black point in Fig. 2)

$P_{L',T',R} = P_{L',T'} \cup P_R$

According to the vehicle direction, determine the entry Point A $(x_{A,g}, y_{A,g})$ and exit Point B $(x_{B,g}, y_{B,g})$ of grid g according to the abscissa or ordinate of the location points in the set $P_{L',T',R}$

Arc length distance between A and B is calculated as $|AB| = \int_{x_{A,g}}^{x_{B,g}} \sqrt{1 + y'(x)^2}\, dx$, where $y(x)$ is the outer boundary function of the route

If $v_{i,g,A} = V_M$, the vehicle has attained the maximum speed upon arriving at Point A, and it travels at a constant speed in section A–B, wherein $v_{i,g,A}$ denotes the speed at which the front of the vehicle reaches point A of the grid (as depicted in case 1 in Fig. 3)

$t_{i,g,B} = t_{i,g,A} + \frac{|AB|}{V_M}$ denotes the time when the vehicle's front arrives at Point B

$v_{i,g,B} = V_M$ indicates the speed at which the vehicle's front arrives at Point B

$t'_{i,g,B} = t_{i,g,A} + \frac{|AB|+d_c}{V_M}$ denotes the time at which the vehicle's rear exits Point B

Else if $v_{i,g,A} < V_M$ and $\frac{{V_M}^2 - {v_{i,g,A}}^2}{2 \cdot a} \geq |AB| + d_c$, the vehicle does not attain the maximum speed upon arriving at Point A and travels at a constant acceleration in section AB (as displayed in case 2 in Fig. 3)

Time when the locomotive arrives at Point B $t_{i,g,B} = t_{i,g,A} + \frac{\sqrt{{v_{i,g,A}}^2 + 2a|AB|} - v_{i,g,A}}{a}$

Speed at which the front reaches Point B $v_{i,g,B} = v_{i,g,A} + a \cdot (t_{i,g,B} - t_{i,g,A})$

Time when the rear of the vehicle exits Point B $t'_{i,g,B} = t_{i,g,A} + \frac{\sqrt{{v_{i,g,A}}^2 + 2a(|AB|+d_c)} - v_{i,g,A}}{a}$

Else If $v_{i,g,A} < V_M$ and $\frac{{V_M}^2 - {v_{i,g,A}}^2}{2 \cdot a} \leq |AB|$, the vehicle does not attain the maximum speed upon arriving at Point A, but operates at a constant speed after constant acceleration within section A–B

if $|AB| - \frac{{V_M}^2 - {v_{i,g,A}}^2}{2 \cdot a} \geq 0$ (as displayed in case 3 of Fig. 3)

Then $t_{i,g,B} = t_{i,g,A} + \frac{|AB| - \frac{{V_M}^2 - {v_{i,g,A}}^2}{2 \cdot a}}{V_M} + \frac{V_M - v_{i,g,A}}{a}$

$v_{i,g,B} = V_M$

Else $t_{i,g,B} = t_{c,g,A} + \frac{\sqrt{{v_{A,g}}^2 + 2a|AB|} - v_{i,g,A}}{a}$ (as displayed in case 4 in Fig. 3)

$v_{i,g,B} = v_{i,g,A} + a \cdot (t_{i,g,B} - t_{i,g,A})$

$t'_{c,g,B} = t_{c,g,A} + \frac{|AB| + d_c - \frac{{V_M}^2 - {v_{i,g,A}}^2}{2 \cdot a}}{V_M} + \frac{V_M - v_{i,g,A}}{a}$

Else vehicles traveling through

Determine the internal and external boundary equations of the vehicle route at the intersection according to the point oblique type straight line equation and calculate the range of x- and y-coordinates

$|AB| = \sqrt{[(x_{B,g} - x_{A,g})^2 + (y_{B,g} - y_{A,g})^2]}$, skip to step 12

End

depending on the routes selected by vehicles to cross the intersection.

To minimize conflicts and improve utilization of the internal intersection zone, we optimized vehicle routes by optimizing the entry and exit lanes. By discretizing the internal intersection zone, we reformulated the issue of conflicts between vehicles at the intersection into the problem of vehicles occupying specific grids. Our objective was to

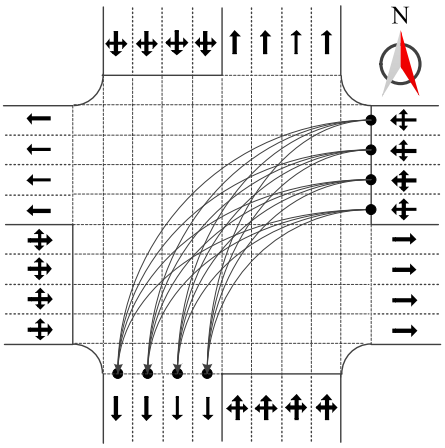

FIGURE 4. Optional routes for left-turning vehicles at east approaching direction.

optimize the lanes for vehicles entering and exiting the intersection in order to minimize the number of vehicles occupying the grids. The modeling procedure is detailed as follows:

Vehicles can select only one route to pass the intersection, as expressed in Equation (1):

$$\sum\nolimits_{r\in R} \Phi_{i,r} = 1 \quad \forall i \in I_n, \tag{1}$$

where I_n is the set of vehicles in the n^{th} time window., r is a route, $r \in R, R$ is the set of all routes, and $\Phi_{i,r}$ is a binary variable indicating whether vehicle i passes the intersection along route r. If $\Phi_{i,r} = 1$, vehicle i passes the intersection from route r; otherwise,$\Phi_{i,r} = 0$.

The entry lane selected by the vehicle is represented as l_i', whereas the selected exit lane is denoted as L_i'. Thus, the selected entry and exit lanes can be determined according to the numbering of the selected route and that of the corresponding entry and exit lanes of each route, as expressed in Equations (2)–(3):

$$l_i' = \sum\nolimits_{r\in R} (\Phi_{i,r} \cdot A_r) \quad \forall i \in I_n \tag{2}$$

$$L_i' = \sum\nolimits_{r\in R} (\Phi_{i,r} \cdot B_r) \quad \forall i \in I_n, \tag{3}$$

where A_r and B_r is the numbering of the entry and exit lanes corresponding to route r, respectively.

The grids comprising each route were determined using the method described in Section IV-A, where $\varphi_{g,o_i,d_i,r}$ denotes a binary variable. If $\varphi_{g,o_i,d_i,r} = 1$, grid g is on route r and can be determined by o_i *and* d_i, and the relationship between the grids on the vehicle route and the route selected by the vehicle is expressed in Equation (4):

$$\sigma_{i,g} = \sum\nolimits_{r\in R} (\Phi_{i,r} \cdot \varphi_{g,o_i,d_i,r}) \quad \forall i \in I_n, g \in G, \tag{4}$$

where $\sigma_{i,g}$ denotes a binary variable indicating whether vehicle i passes through grid g. In case $\sigma_{i,g} = 1$, vehicle i passes through grid g; otherwise, $\sigma_{i,g} = 0$.

Each grid may be used by multiple vehicles. The total number Ω_g of vehicles clear grid g at any given time is calculated using Equation (5):

$$\Omega_g = \sum\nolimits_{i\in I_n} \sigma_{i,g} \quad \forall g \in G \tag{5}$$

The number of vehicles in the most frequently used grid is calculated using Equation (6):

$$\Omega = \max_{g\in G} \Omega_g \tag{6}$$

where Ω is the number of vehicles in the most occupied grid.

In [22], a centralized and coordinated method for intersection control is proposed, aiming to minimize the overall length of overlapping vehicle trajectories; however, it does not optimize the routes of vehicles within the intersection. Upon discretizing the internal zone of the intersection into multiple grids, the traversal routes of vehicles inside the intersection can be expressed as a series of grids. In this study, we present a novel approach of route overlap planning, whereby the problem is reframed as a determination of the number of vehicles clearing each grid. By minimizing the number of vehicles clear each grid, we aim to reduce the overlap of routes at intersections, which in turn ensures minimal conflict between vehicles. The optimization objective of the route planning model is expressed as Equation (7):

$$min(\max_{g\in G} \Omega_g) \tag{7}$$

C. TRAFFIC CONTROL MODEL

Although the route optimization model effectively minimizes conflicts between vehicles at intersections, however, achieving complete separation of all potential conflicts requires further optimization of the sequencing and timing of vehicle entry as determined by the lower-level traffic control model. The traffic control model takes the results of route optimization from section IV-B as input and optimizes the times of vehicle entry into the intersection with the aim of minimizing total vehicle delay. This model is subject to three primary constraints: the intersection arrival time constraint, the grid entering and exiting time constraint, and the conflict separation constraint.

1) INTERSECTION ARRIVAL TIME CONSTRAINTS

Considering the operation of vehicles, T_i'', the instant at which vehicles actually enter the intersection, is not less than T_i', the instant at which the vehicles actually arrive at the intersection, and T_i' is not less than T_i, the instant at which the vehicle planed arrives at the intersection. The constraint is expressed in Equation (8):

$$T_i'' \geq T_i' \geq T_i \quad \forall\, i \in I. \tag{8}$$

There are two scenarios for vehicles: those that come to a stop before entering the intersection and those that do not. If the vehicle stops before entering the intersection, the actual time the vehicle entering the intersection is greater than the planed time of its arrival at the intersection, *i.e.*, $T_i'' > T_i$; otherwise,

$T_i^{''} = T_i$. The relationship between $T_i^{''}$ and T_i is expressed in Equation (9):

$$If \quad \rho_{0,i} = 1 \quad then\ T_i^{''} > T_i \ \ else\ T_i^{''} = T_i. \tag{9}$$

By linearizing Equation (9), the instants of the vehicle actually entering the intersection and planned arriving at the intersection should satisfy the following equations:(10) –(11)

$$T_i^{''} > T_i - M \cdot (1 - \rho_{0,i}) \quad \forall i \in I \tag{10}$$

$$T_i^{''} \leq T_i + M \cdot \rho_{0,i} \quad \forall i \in I. \tag{11}$$

2) GRID ENTERING AND EXITING TIME CONSTRAINT

The timespan between the entry and exit of the vehicle from the grid can be determined based on the time $T_i^{''}$ when the vehicle enters the intersection, and the time required by the vehicle to cross the intersection, where $T_i^{''}$ is the decision variable of the traffic control model. The time at which the vehicle passes any grid on the route has been calculated in Section IV-A. The time $T_{i,g}$ at which the vehicle enters the grid should follow the conditions expressed in Equations (12)–(13):

$$T_{i,g} \geq T_i^{''} + t_{g,r_i,v} \cdot \cdot \rho_{0,i} - M_1 \cdot (1 - \sigma_{i,g}), \tag{12}$$

$$T_{i,g} \leq T_i^{''} + t_{g,r_i,v} \cdot \rho_{v,i} + M_1 \cdot (1 - \sigma_{i,g}). \tag{13}$$

The time $T'_{i,g}$ at which the vehicle exits the grid should suffice the conditions presented in Equation (14)-(15):

$$T'_{i,g} \geq T_i^{''} + t'_{g,r_i,v} \cdot \rho_{v,i} - M_1 \cdot (1 - \sigma_{i,g}), \tag{14}$$

$$T'_{i,g} \leq T_i^{''} + t'_{g,r_i,v} \cdot \rho_{v,i} + M_1 \cdot (1 - \sigma_{i,g}), \tag{15}$$

where $t_{g,r_i,v}$ and $t'_{g,r_i,v}$ is the time at which the front of the vehicle i enters grid g and the time at which the tail of vehicle i exits grid g after the vehicle enters the intersection, respectively.

To address the complexity associated with calculating the time of a vehicle entering and leaving an intersection due to the continuous nature of vehicle speeds, it is necessary to discretize the speed variable. This discretization restricts the vehicle's options for entering the intersection to a finite set. The vehicle can only select a certain speed to enter the intersection. The constraint is expressed in Equation (16).

$$\sum\nolimits_{v \in V} \rho_{v,i} = 1 \tag{16}$$

where, V represent the set of discretized speeds, i.e., $V = \{0, \ldots, V_m\}$.

3) CONFLICT SEPARATION CONSTRAINT

To ensure the safe passage of vehicles at intersections, prior studies have assumed that each grid can be occupied by only one vehicle at any given time. When multiple vehicles pass through a grid two or more times, temporal separation is required to prevent collisions. To address this issue, we formed conflict sets $\{(g, i, j), \ldots\}$, and then formulated constraints (17)–(18) to ensure that the entry and exit times of each vehicle pair did not overlap. Notably, unlike [33], which investigated all vehicles under a discrete grid set, we only conducted conflict separation on grids traversed by two or more vehicles, thereby eliminating redundant solutions and effectively reducing the size of the solution space. The conflict separation constraint is expressed in Equations (17) –(18).

$$T'_{i,g} - T_{j,g} \leq M \cdot y_{i,j} \quad \forall g, i, j \in \{(g, i, j), \ldots\} \tag{17}$$

$$T'_{j,g} - T_{i,g} \leq M \cdot \left(1 - y_{i,j}\right) \quad \forall g, i, j \in \{(g, i, j), \ldots\}, \tag{18}$$

where $y_{i,j}$ is a binary variable. In case $y_{i,j} = 1$, vehicle j enters the same grid before vehicle i, whereas $y_{i,j} = 0$ is that vehicle i enters the same grid before vehicle j. The conflict set $\{(g, i, j), \ldots\}$ was calculated following the method described in Section IV-B.

The delay of all vehicles was calculated using Equation (19):

$$D_I = \sum\nolimits_{i \in I} (T_i^{''} - T_i). \tag{19}$$

The lower-level traffic control model aims to minimize the delay of vehicles at the intersection, and the objective function is expressed in Equation (20):

$$\min D_I. \tag{20}$$

V. MODEL SOLUTION

Although vehicles arriving at the intersection at different times may have potential conflicts, actual conflicts may not occur when the time difference of their arrival at the intersection is significant. Therefore, the rolling time window method is used [31]. Specifically, we segmented various time windows based on the arrival times of vehicles at the intersection to optimize their routes and entry times. If the entry time of any vehicle in the subsequent time window is later than or equal to the latest exit time for all vehicles in the previous time window, we must satisfy the conditions outlined in Equation (21):

$$T_{k,g} \geq \max_{i \in I_n} \left\{T'_{i,g}\right\} \cdot \sigma_{i,g} \quad \forall g \in G, k \in I_{n+1}, \tag{21}$$

where I_n is the set of vehicles in the n^{th} time window.

The upper- and lower-level models were both mixed-integer linear programming models that can be solved using the branch and bound method. The model is described as follows:

The upper-level models:
Decision variables: l'_i, L'_i, $\sigma_{i,g}$
Objective function: $min(\max_{g \in G} \Omega_g)$
Constraint conditions: Equations (1)–(6).
The lower-level models:
Decision variables: $T_i^{''}$, $\Phi_{i,r}$, $\rho_{v,i}$, $y_{i,j}$
Objective function:min D_I
Constraint conditions: Equations (8)–(19).

In order to calculate the timing of vehicle entry and exit for each grid, we utilized Python programming to solve our calculation model in Section IV-A. The route optimization and traffic control models were formulated and encoded using

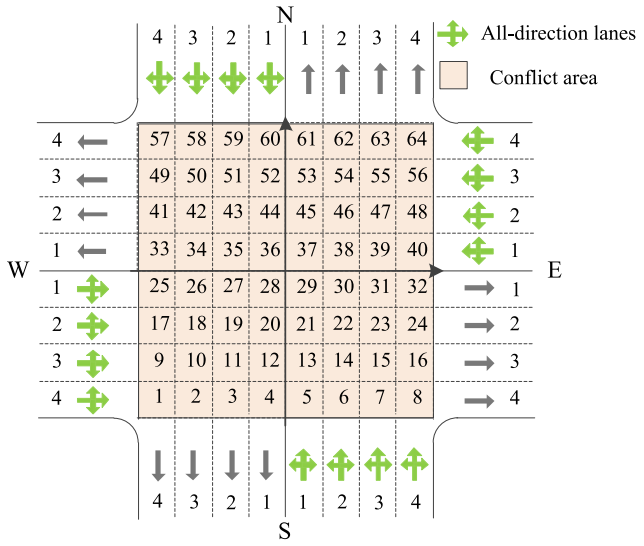

FIGURE 5. The layout of the intersection.

AMPL, a well-established optimization modeling software, and solved using CPLEX, a widely adopted solver for linear and integer programming. Notably, the CPLEX solver, developed by IBM, is renowned for its exceptional efficiency in solving complex optimization problems [39].

VI. MODEL VERIFICATION AND BENEFIT ANALYSIS

In this Section, we selected the intersection of Fu Rong Road and Ying Pan Road in Changsha, China, which encompasses eight lanes in each direction and allows bi-directional traffic flow. Fig. 5 illustrates that the entry and exit lanes in all directions of the intersection were clearly numbered, each with a width of $d_l = 3.5$m. Grid granularity significantly impacts intersection efficiency [40]. The grid's side length should not be set to very large, e.g., if the whole intersection is taken as a single grid, this means only one vehicle can be inside the intersection at a time, which would certainly cause massive efficiency losses. Therefore, in order to take better advantage of the space inside the intersection, the side length of a grid is better shorter than the vehicle length and larger than zero. However, smaller side length correspond to more numbers of girds, and because all the conflicts on each gird should be avoided, more numbers of girds lead to more computational time. By following Wu et al. (2022), the grid dimension is set to 3.5 m * 3.5 m in this study. The vehicles involved in this study had a length of $d_c = 4.5m$ and a maximum speed of $V_M = 16.7$ m/s (60km/h) when passing through the intersection. To ensure passenger comfort, the maximum acceleration of the AV was limited to $a = 2.5\text{m/s}^2$. The arrival of vehicles at the intersection followed the Poisson distribution. The average time headway per entrance lane between two successive vehicles is 3.75 seconds, which is equivalent to 960 vehicles per hour per entrance lane. Given that there are 16 entrance lanes, the average arrival rate at the intersection is approximately 4.27 vehicles per second.

Based on the planned arrival time, we categorized the vehicles into time windows of 10 seconds [33]. The proposed model utilized a desktop computer equipped with a Windows 10 (64-bit) system, featuring an Intel (R) CoreTM i5-9400F processor clocked at 2.90 GHz and 8 GB of memory. To ensure the efficiency of solving, we set the maximum solving time at 10 seconds, i.e., if the optimal solution cannot be obtained within 10 seconds, the solver will return the best feasible solution derived within 10 seconds.

In this study, the global optimization (GO) model optimized the vehicle routes, the order and the time of entering the intersection. To assess the effectiveness of the proposed model, we have developed several comparison models to use in our analysis.

To demonstrate the effectiveness of route optimization, we utilized the global optimum method without route choices (GO-WR) as the comparison model. Unlike the proposed model, GO-WR did not optimize the vehicle routes at the intersection. Instead, it focused on optimizing the timing of the vehicles entering the intersection. The route was determined based on the initial entry and exit lanes provided as inputs.

In addition, we employed the first-come-first-served with optimal route choices (FCFS-R) method to compare the effects of optimizing the time of vehicles entering the intersection. The FCFS-R model used the same optimization method for vehicle routes inside the intersection as the proposed model. However, the order of vehicles entering the intersection followed the first-come-first-serve rule, meaning that the vehicles entered the intersection according to the sequence of their arrival, and the time of vehicles entering the intersection was not optimized.

The application of the GO model effectively reduced the number of conflicts between vehicles in each time window when compared to the GO-WR model. As illustrated in Fig. 6, during the first, second, and third time windows, the GO-WR model recorded 2,237, 1,940, and 2,363 conflicts, respectively. In contrast, with GO model, the conflicts reduced to 865, 908, and 906, respectively, which represents a significant decrease of 61.33%, 53.2%, and 61.66%, respectively. The results demonstrate the effectiveness of the proposed model in reducing the conflicts between vehicles at intersections.

In addition, the time at which the vehicles entered the intersection was recorded to determine the delay experienced by the vehicles passing through the intersection in each time window. The delay comparison is illustrated in Fig. 7.

Three conclusions can be drawn from the results presented in Fig. 7. First, It can be observed that the blue box corresponding to the GO model results occupied the lowest position and spanned the shortest length compared to those of the GO-WR and FCFS-R models. This indicates that the GO model has shorter delay. Second, the average vehicle delay in the GO model for the three time windows was 1.79 s, 4.32 s, and 6.71 s, respectively, while that in the GO-WR model was 6.99 s, 14.18 s, and 21.80 s, respectively. Compared

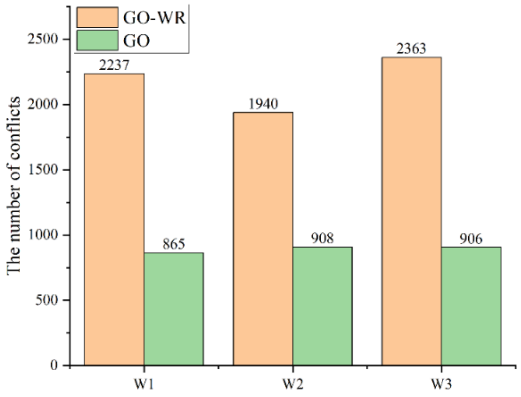

FIGURE 6. The comparison of the number of conflicts.

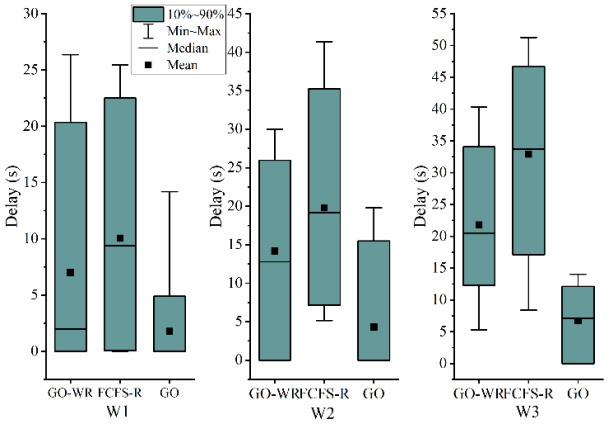

FIGURE 7. The comparison of vehicle delays.

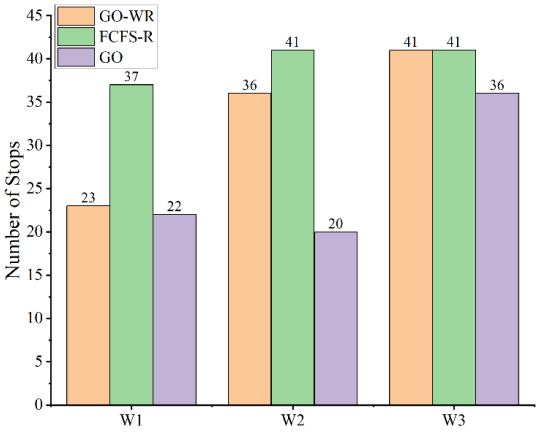

FIGURE 8. The number of stops.

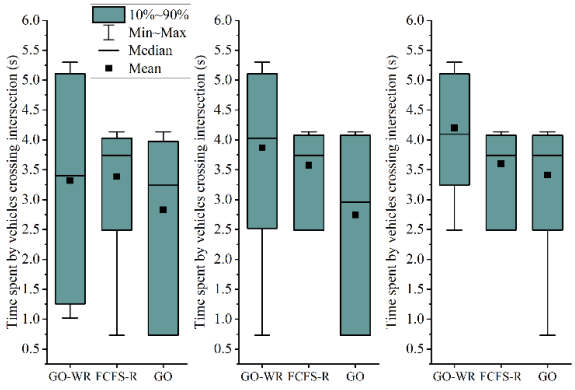

FIGURE 9. Time spent by vehicles crossing intersection.

with the GO-WR model, the average vehicle delay in the GO model was reduced by 74.43%, 69.51%, and 69.22%, respectively. This suggests that minimizing the number of vehicles clearing grid can optimize the vehicle trajectory, reduce conflicts between vehicles, thus effectively reducing vehicle delay. Finally, the average vehicle delay of the FCFS-R model for the three time windows was 10.06 s, 19.79 s, and 32.91s s, which further reduced the average vehicle delay of the GO model by 82.22%, 78.16%, and 79.61%, respectively. This finding indicates that optimizing the time of the vehicles entering the intersection can significantly reduce vehicle delay. The number of stops before the vehicle entering the intersection is shown in Fig. 8.

According to Fig. 8, there is a significant decrease in the total number of vehicle stops in the proposed model across different time windows. Specifically, in comparison to the GO-WR model, the GO model demonstrated a reduction of 4.35%, 40.54%, and 44.44% in the total number of stops, respectively. Additionally, when compared with FCFS-R, the GO model exhibited a decrease of 51.22%, 12.20%, and 12.20%, respectively. The time spent by vehicles crossing intersection is shown in Fig. 9.

Fig. 9 revealed that the time spent by vehicles crossing intersection in the GO model was significantly shorter than those in the GO-WR and FCFS-R models. During the three time windows, the GO model resulted in average occupation times of 2.83 s, 2.75 s, and 3.41 s, respectively, while the corresponding values for the GO-WR model were 3.32 s, 3.87 s, and 4.20 s, respectively. This results in a reduction of 14.74%, 29.01%, and 18.72% in average occupation time when comparing GO and GO-WR. Moreover, the average occupation time in FCFS-R was 3.39 s, 3.58 s, and 3.60 s, respectively, which is longer than that of the GO model by 16.53%, 23.22%, and 5.28%, respectively.

The results indicate that optimizing vehicle routes and the time of entering the intersection can significantly reduce the time spent by vehicles crossing intersection. This is due to optimized routes and reduced travel time, resulting in fewer vehicle conflicts and less frequent stops by vehicles at the intersection. The average speed of vehicles traveling through the intersection increases, and time spent inside the intersection is decreased.

Fig. 10 presents the vehicle count clear each grid at the intersection, which shows a more evenly distributed conflict distribution among the vehicles following the vehicle route optimization approach. Notably, the proposed approach resulted in a significant reduction in the number of vehicles clear each grid. For instance, during time window 1, the maximum number of vehicles clear a single grid in the model

FIGURE 10. Number of vehicles passed by each grid.

was seven, while in the comparison model without route optimization, 15 vehicles passed through a same grid. This result suggests that the vehicle route optimization approach promotes a more equitable distribution of spatial resource utilization at the intersection.

Fig. 11 shows vehicles' trajectories within the intersection across different time windows. While this study incorporates vehicle size and represents their trajectories using enclosed regions defined by inner and outer boundaries, the figure portrays the centerline of the trajectories for clarity purposes. From Fig. 11, it is evident that the FCFS-R model, which does not optimize vehicles' routes within the intersection, results in chaotic vehicle trajectories with numerous instances of trajectory crossings. However, by employing the proposed

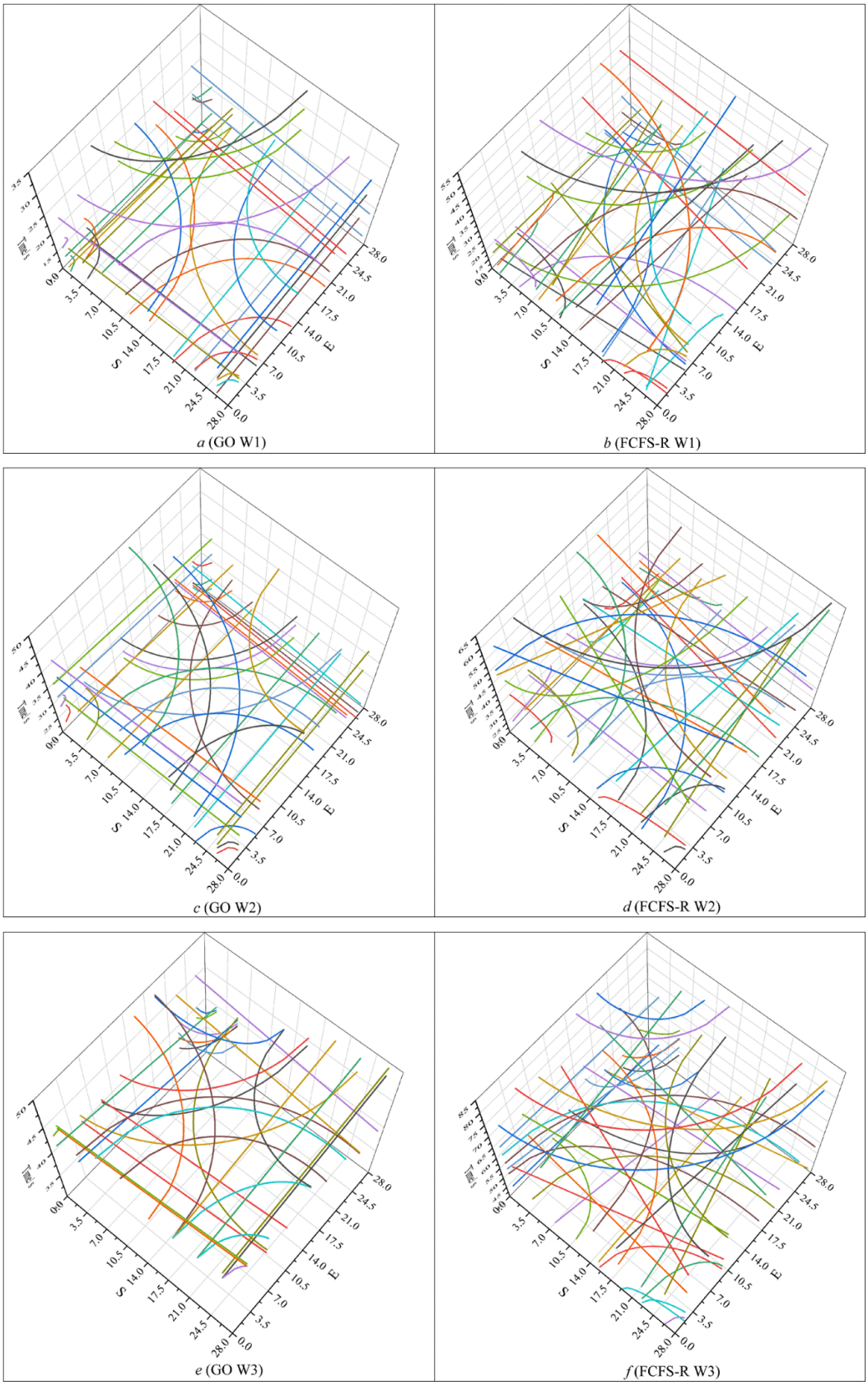

FIGURE 11. Vehicles' trajectories.

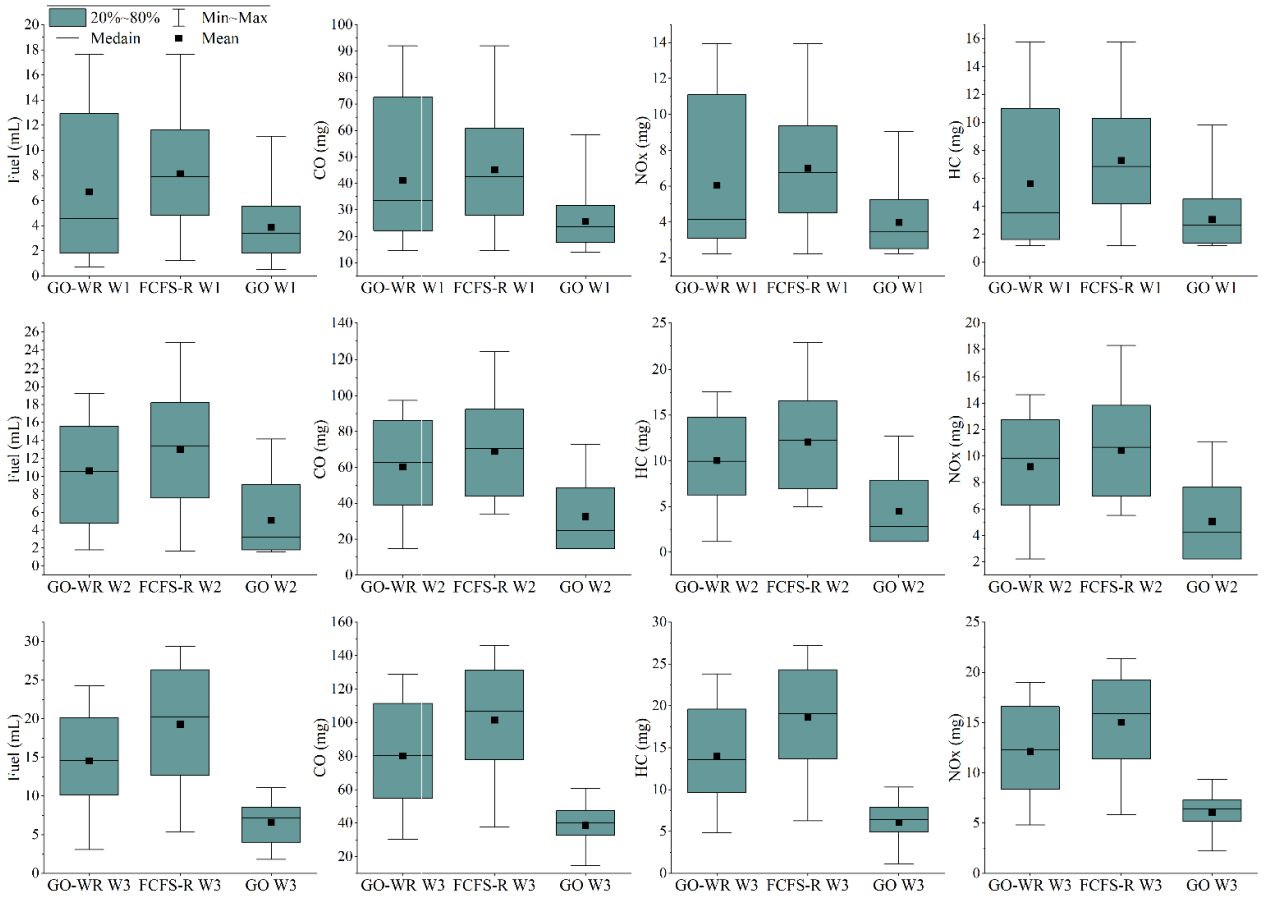

FIGURE 12. Fuel consumption and pollutant emission of vehicles.

model, a more structured distribution of trajectories is achieved.

As shown in Fig. 11, in different time windows, the predominant behavior observed in vehicle trajectories can be summarized as follows: the majority of left-turning vehicles tend to opt for inner lanes, exemplified by Lane 1 or Lane 2 in Fig. 5, while right-turning vehicles typically prefer outer lanes, such as Lane 3 or Lane 4 in Fig. 5. Specifically, within the time windows, left-turning vehicles displayed distribution of 16.7%, 25%, and 25% for selecting Entrance Lanes 3 or Lanes 4, respectively. Meanwhile, right-turning vehicles exhibited proportions of 8.33%, 16.67%, and 15.38% for choosing Entrance Lanes 1 or Lanes 2 in the respective time windows. On the other hand, the selection of entrance lanes by through-traffic vehicles did not demonstrate a discernible pattern. The analysis of the vehicle's choice of exit lane shows that within the different time windows, the proportion of vehicles following a circular turning trajectory is 75.00%, 95.83%, and 88.00%, respectively. Furthermore, all straight trajectories parallel to the x-axis or y-axis.

As demonstrated by the analysis presented above, our proposed model has exhibited a significant reduction in both vehicle conflicts and delays. Given the transportation industry's increasing concern with energy consumption and pollutant emissions, considerable efforts have been made towards traffic control systems that prioritize energy conservation and emission reduction [41]. In line with this, we have evaluated the energy consumption and pollutant emissions of vehicles passing through intersections, utilizing the fuel consumption model to determine the impact of our proposed model on these factors. Specifically, we have employed the VT-Micro model, which efficiently calculates fuel consumption and emissions of carbon oxide (CO), nitrogen oxide (NO_X), and carbon hydride (HC) based on vehicle speed and acceleration, as outlined in Equations (22) –(23). The regression coefficient values for these equations are detailed in Appendix, and Fig. 12 presents the calculated fuel consumption and emissions of CO, HC, and NO_X for all vehicles across the three time windows.

$$MOE_{fuel} = \sum_{t=0}^{T} \exp\left(\sum_{i=0}^{3}\sum_{j=0}^{3} k_{i,j}^{e} \cdot v(t)^{i} \cdot a(t)^{j}\right)/3.6, e = fuel \quad (22)$$

$$MOE_{e} = \sum_{t=0}^{T} \exp\left(\sum_{i=0}^{3}\sum_{j=0}^{3} k_{i,j}^{e} \cdot v(t)^{i} \cdot a(t)^{j}\right), \quad \forall e \in \{CO, HC, NOx\} \quad (23)$$

TABLE 3. Mean values of fuel consumption and pollutant emission from vehicles at different time windows.

Time window	Model	Fuel (mL)	CO (mg)	HC (mg)	NOx (mg)
W1	GO-WR	7.14	42.35	5.91	6.28
	FCFS-R	8.66	46.38	7.53	7.17
	GO	4.11	26.03	3.17	4.08
W2	GO-WR	11.10	59.03	9.77	9.01
	FCFS-R	13.73	70.25	12.37	10.62
	GO	5.35	32.02	4.35	4.95
W3	GO-WR	15.24	78.73	13.69	11.91
	FCFS-R	20.27	101.37	18.63	14.99
	GO	6.91	37.73	5.89	5.96

Compared to GO-WR and FCFS-R, the GO model exhibited a significant reduction in both fuel consumption and pollutant emission for vehicles passing through the intersection. Table 3 displays the average fuel consumption and pollutant emissions for all vehicles during the three time windows. The average reduction in fuel consumption and pollutant emissions ranged from 35 to 68%.

VII. CONCLUSION

Traffic signal control at intersections presents significant challenges, which include the suboptimal utilization of traffic efficiency. Such suboptimal utilization results from issues such as wastage of green light time and loss of phase switching time. These problems impede the efficient functioning of intersections and require innovative solutions. In autonomous environments, vehicles have the potential to traverse intersections without the need for traditional signal control by utilizing AIM. This innovative approach promotes the smooth flow of traffic, thereby enhancing the utilization of space-time resources at intersections. Based on AIM, every entry lane at the intersection has the capability to serve as left-turn, through, and right-turn routes, resulting in an increased number of route options for vehicles traverse the intersection. This feature allows for a more versatile and efficient use of the available space, enhancing the overall performance of the intersection. As the location and dimensions of the conflict zones differ for each route, optimizing vehicle routes at the intersection can be instrumental in reducing traffic conflicts and enhancing traffic efficiency. By customizing routes planning for each vehicle, it is possible to minimize the likelihood of conflicts and promote a more streamlined flow of traffic at the intersection. Most existing AIM models adopt predetermined routes for AVs and treat them as exogenous inputs, directing attention towards conflicts that arise at intersections. Additionally, these models assume a constant speed for AVs and neglect the possibility of stops during intersection traversal. However, this is not practically possible in case of heavy traffic flow.

The present study establishes a time calculation model for vehicles entering and exiting an intersection grid, enabling accurate estimation of traversal time for vehicles crossing the grids of the intersection. Second, a bi-level programming model is proposed in this study, which involves an upper-level model for optimizing vehicle routes at intersections and a lower-level model for optimizing entry time of vehicles, thereby mitigating potential conflicts between them. The model was solved using Python and AMPL. The outcomes of our study demonstrate that, by route optimization, the number of conflicts between vehicles was reduced significantly. This impressive decrease of over 50% stands in stark contrast to the GO-WR model which without route optimization. The results suggest that the proposed model is effective in optimizing travel routes for vehicles at intersections. Furthermore, the optimization ensures a more uniform distribution of conflict points within the intersection, ultimately leading to an improved utilization of space resources at intersections. In comparison to the GO-WR model, the proposed route optimization model results in a significant reduction of vehicle delay, ranging between 69-74%. The model reduces the number of stopping vehicles by 4-44%, and reduces the time spent by vehicles crossing intersection by 14-29%. Notably, the proposed model enables evaluation of fuel consumption and pollutant emissions during vehicle operation based on trajectory data, resulting in a mean reduction of 35-68%. These findings confirm the feasibility and effectiveness of the model. More importantly, the model is capable of reducing the fuel consumption and pollutant emissions of vehicles while reducing vehicle delay and improving the traffic efficiency at intersections.

Moreover, the present study offers potential avenues for further research, including but not limited to the following zones: First, future research may consider the formation of vehicle platoon for modeling and optimization, as demonstrated in previous studies [42]. Furthermore, it may be worthwhile to investigate scenarios that involve both pedestrians and AVs simultaneously [43]. Additionally, developing a simulation platform to validate the control effect of the proposed model can also be further expanded in the following studies [44]. Furthermore, future research can explore the implementation of a distributed traffic control approach, allowing autonomous vehicles to autonomously plan and adapt their trajectories in real-time [45]. Lastly, with the ongoing rapid development of new energy vehicles and their increasing prevalence, it is imperative for forthcoming studies to address the changing energy consumption dynamics in these vehicles. This necessitates the establishment of energy

TABLE 4. Regression coefficients in the fuel consumption model.

Parameters	Fuel	CO	HC	NOx
$k^A_{0,0}$	−0.679439	0.887447	−0.728042	−1.067682
$k^A_{0,1}$	0.135273	0.148841	0.012211	0.254363
$k^A_{0,2}$	0.015946	0.03055	0.023371	0.008866
$k^A_{0,3}$	−0.001189	−0.001348	−0.000093243	−0.000951
$k^A_{1,0}$	0.029665	0.070994	0.02495	0.046423
$k^A_{1,1}$	0.004808	0.00387	0.010145	0.015482
$k^A_{1,2}$	−0.000020535	0.000093228	−0.000103	−0.000131
$k^A_{1,3}$	5.5409285E-8	−0.000000706	0.000000618	0.000000328
$k^A_{2,0}$	−0.000276	−0.000786	−0.000205	−0.000173
$k^A_{2,1}$	0.000083329	−0.000926	−0.000549	0.002876
$k^A_{2,2}$	0.000000937	0.000049181	0.000037592	−0.00005866
$k^A_{2,3}$	−2.479644E-8	−0.000000314	−0.000000213	0.00000024
$k^A_{3,0}$	0.000001487	0.000004616	0.000001949	0.000000569
$k^A_{3,1}$	−0.000061321	0.000046144	−0.000113	−0.000321
$k^A_{3,2}$	0.000000304	−0.00000141	0.00000331	0.000001943
$k^A_{3,3}$	−4.467234E–9	8.1724008E–9	−1.739372E–8	−1.257413E–8

consumption models explicitly designed for new energy vehicles, as the VT-Micro model used in this study for conventional fuel vehicles is not applicable in this context.

APPENDIX
PARAMETERS OF REGRESSION COEFFICIENT

See table 4.

REFERENCES

[1] A. Gholamhosseinian and J. Seitz, "A comprehensive survey on cooperative intersection management for heterogeneous connected vehicles," *IEEE Access*, vol. 10, pp. 7937–7972, 2022, doi: 10.1109/ACCESS.2022.3142450.

[2] K. Long, C. Ma, Z. Jiang, Y. Wang, and X. Yang, "Integrated optimization of traffic signals and vehicle trajectories at intersection with the consideration of safety during signal change," *IEEE Access*, vol. 8, pp. 170732–170741, 2020, doi: 10.1109/ACCESS.2020.3021082.

[3] C. Yu, W. Ma, H. K. Lo, and X. Yang, "Robust optimal lane allocation for isolated intersections," *Comput.-Aided Civil Infrastruct. Eng.*, vol. 32, no. 1, pp. 72–86, Jan. 2017, doi: 10.1111/mice.12236.

[4] W. Wu, Y. Liu, W. Liu, F. Zhang, D. Rey, and V. Dixit, "An integrated approach for optimizing left-turn forbiddance decisions at multiple intersections," *Transportmetrica B, Transp. Dyn.*, vol. 7, no. 1, pp. 1481–1504, Dec. 2019, doi: 10.1080/21680566.2019.1631901.

[5] Q. Luo, J. Yuan, X. Chen, S. Wu, Z. Qu, and J. Tang, "Analyzing start-up time headway distribution characteristics at signalized intersections," *Phys. A, Stat. Mech. Appl.*, vol. 535, Dec. 2019, Art. no. 122348, doi: 10.1016/j.physa.2019.122348.

[6] Y. Wei, C. Avcı, J. Liu, B. Belezamo, N. Aydın, P. Li, and X. Zhou, "Dynamic programming-based multi-vehicle longitudinal trajectory optimization with simplified car following models," *Transp. Res. B, Methodol.*, vol. 106, pp. 102–129, Dec. 2017, doi: 10.1016/j.trb.2017.10.012.

[7] L. Chen and C. Englund, "Cooperative intersection management: A survey," *IEEE Trans. Intell. Transp. Syst.*, vol. 17, no. 2, pp. 570–586, Feb. 2016, doi: 10.1109/TITS.2015.2471812.

[8] K. Dresner and P. Stone, "Multiagent traffic management: A reservation-based intersection control mechanism," in *Proc. 3rd Int. Joint Conf. Auton. Agents Multiagent Syst.*, vol. 3, Jul. 2004, pp. 530–537.

[9] K. Dresner and P. Stone, "A multiagent approach to autonomous intersection management," *J. Artif. Intell. Res.*, vol. 31, pp. 591–656, Mar. 2008, doi: 10.1613/jair.2502.

[10] S. Huang, A. W. Sadek, and Y. Zhao, "Assessing the mobility and environmental benefits of reservation-based intelligent intersections using an integrated simulator," *IEEE Trans. Intell. Transp. Syst.*, vol. 13, no. 3, pp. 1201–1214, Sep. 2012, doi: 10.1109/TITS.2012.2186442.

[11] G. Lu, Z. Shen, X. Liu, Y. M. Nie, and Z. Xiong, "Are autonomous vehicles better off without signals at intersections? A comparative computational study," *Transp. Res. B, Methodol.*, vol. 155, pp. 26–46, Jan. 2022, doi: 10.1016/j.trb.2021.10.012.

[12] Z. Deng, Y. Shi, Q. Han, L. Lv, and W. Shen, "A conflict duration graph-based coordination method for connected and automated vehicles at signal-free intersections," *Appl. Sci.*, vol. 10, no. 18, p. 6223, Sep. 2020, doi: 10.3390/app10186223.

[13] X. Chen, M. Hu, B. Xu, Y. Bian, and H. Qin, "Improved reservation-based method with controllable gap strategy for vehicle coordination at non-signalized intersections," *Phys. A, Stat. Mech. Appl.*, vol. 604, Oct. 2022, Art. no. 127953, doi: 10.1016/j.physa.2022.127953.

[14] C. Wuthishuwong, A. Traechtler, and T. Bruns, "Safe trajectory planning for autonomous intersection management by using vehicle to infrastructure communication," *EURASIP J. Wireless Commun. Netw.*, vol. 2015, no. 1, pp. 1–12, Feb. 2015, doi: 10.1186/s13638-015-0243-3.

[15] B. Liu, Q. Shi, Z. Song, and A. El Kamel, "Trajectory planning for autonomous intersection management of connected vehicles," *Simul. Model. Pract. Theory*, vol. 90, pp. 16–30, Jan. 2019, doi: 10.1016/j.simpat.2018.10.002.

[16] Y. Zhang, L. Liu, Z. Lu, L. Wang, and X. Wen, "Robust autonomous intersection control approach for connected autonomous vehicles," *IEEE Access*, vol. 8, pp. 124486–124502, 2020, doi: 10.1109/ACCESS.2020.3002825.

[17] J. Wu, F. Perronnet, and A. Abbas-Turki, "Cooperative vehicle-actuator system: A sequence-based framework of cooperative intersections management," *IET Intell. Transp. Syst.*, vol. 8, no. 4, pp. 352–360, Jun. 2014, doi: 10.1049/iet-its.2013.0093.

[18] A. Mirheli, L. Hajibabai, and A. Hajbabaie, "Development of a signal-head-free intersection control logic in a fully connected and autonomous vehicle environment," *Transp. Res. C, Emerg. Technol.*, vol. 92, pp. 412–425, Jul. 2018, doi: 10.1016/j.trc.2018.04.026.

[19] Z. Li, Q. Wu, H. Yu, C. Chen, G. Zhang, Z. Z. Tian, and P. D. Prevedouros, "Temporal–spatial dimension extension-based intersection control formulation for connected and autonomous vehicle systems," *Transp. Res. C, Emerg. Technol.*, vol. 104, pp. 234–248, Jul. 2019, doi: 10.1016/j.trc.2019.05.003.

[20] A. A. Malikopoulos, C. G. Cassandras, and Y. J. Zhang, "A decentralized energy-optimal control framework for connected automated vehicles at signal-free intersections," *Automatica*, vol. 93, pp. 244–256, Jul. 2018, doi: 10.1016/j.automatica.2018.03.056.

[21] Z. Yao, H. Jiang, Y. Cheng, Y. Jiang, and B. Ran, "Integrated schedule and trajectory optimization for connected automated vehicles in a conflict zone," *IEEE Trans. Intell. Transp. Syst.*, vol. 23, no. 3, pp. 1841–1851, Mar. 2022, doi: 10.1109/TITS.2020.3027731.

[22] Z. Wu and B. Waterson, "Urban intersection management strategies for autonomous/connected/conventional vehicle fleet mixtures," *IEEE Trans. Intell. Transp. Syst.*, vol. 23, no. 8, pp. 12084–12093, Aug. 2022, doi: 10.1109/TITS.2021.3109783.

[23] J. Rios-Torres and A. A. Malikopoulos, "A survey on the coordination of connected and automated vehicles at intersections and merging at highway on-ramps," *IEEE Trans. Intell. Transp. Syst.*, vol. 18, no. 5, pp. 1066–1077, May 2017, doi: 10.1109/TITS.2016.2600504.

[24] Y. Bian, S. E. Li, W. Ren, J. Wang, K. Li, and H. X. Liu, "Cooperation of multiple connected vehicles at unsignalized intersections: Distributed observation, optimization, and control," *IEEE Trans. Ind. Electron.*, vol. 67, no. 12, pp. 10744–10754, Dec. 2020, doi: 10.1109/TIE.2019.2960757.

[25] L. Li and F.-Y. Wang, "Cooperative driving at blind crossings using intervehicle communication," *IEEE Trans. Veh. Technol.*, vol. 55, no. 6, pp. 1712–1724, Nov. 2006, doi: 10.1109/TVT.2006.878730.

[26] H. Xu, Y. Zhang, L. Li, and W. Li, "Cooperative driving at unsignalized intersections using tree search," *IEEE Trans. Intell. Transp. Syst.*, vol. 21, no. 11, pp. 4563–4571, Nov. 2020, doi: 10.1109/TITS.2019.2940641.

[27] W. Wu, J. Zhang, A. Luo, and J. Cao, "Distributed mutual exclusion algorithms for intersection traffic control," *IEEE Trans. Parallel Distrib. Syst.*, vol. 26, no. 1, pp. 65–74, Jan. 2015, doi: 10.1109/TPDS.2013.2297097.

[28] G. Rodrigues de Campos, P. Falcone, R. Hult, H. Wymeersch, and J. Sjöberg, "Traffic coordination at road intersections: Autonomous decision-making algorithms using model-based heuristics," *IEEE Intell. Transp. Syst. Mag.*, vol. 9, no. 1, pp. 8–21, Jan. 2017, doi: 10.1109/MITS.2016.2630585.

[29] C. Liu, C.-W. Lin, S. Shiraishi, and M. Tomizuka, "Distributed conflict resolution for connected autonomous vehicles," *IEEE Trans. Intell. Vehicles*, vol. 3, no. 1, pp. 18–29, Mar. 2018, doi: 10.1109/TIV.2017.2788209.

[30] A. Katriniok, B. Rosarius, and P. Mähönen, "Fully distributed model predictive control of connected automated vehicles in intersections: Theory and vehicle experiments," *IEEE Trans. Intell. Transp. Syst.*, vol. 23, no. 10, pp. 18288–18300, Oct. 2022, doi: 10.1109/TITS.2022.3162038.

[31] M. W. Levin and D. Rey, "Conflict-point formulation of intersection control for autonomous vehicles," *Transp. Res. C, Emerg. Technol.*, vol. 85, pp. 528–547, Dec. 2017, doi: 10.1016/j.trc.2017.09.025.

[32] Z. Yao, H. Jiang, Y. Jiang, and B. Ran, "A two-stage optimization method for schedule and trajectory of CAVs at an isolated autonomous intersection," *IEEE Trans. Intell. Transp. Syst.*, vol. 24, no. 3, pp. 3263–3281, Mar. 2023, doi: 10.1109/TITS.2022.3230682.

[33] W. Wu, Y. Liu, W. Liu, F. Zhang, V. Dixit, and S. T. Waller, "Autonomous intersection management for connected and automated vehicles: A lane-based method," *IEEE Trans. Intell. Transp. Syst.*, vol. 23, no. 9, pp. 15091–15106, Sep. 2022, doi: 10.1109/TITS.2021.3136910.

[34] Z. He, L. Zheng, L. Lu, and W. Guan, "Erasing lane changes from roads: A design of future road intersections," *IEEE Trans. Intell. Vehicles*, vol. 3, no. 2, pp. 173–184, Jun. 2018, doi: 10.1109/tiv.2018.2804164.

[35] H. Jiang, Z. Yao, Y. Jiang, and Z. He, "Is all-direction turn lane a good choice for autonomous intersections? A study of method development and comparisons," *IEEE Trans. Veh. Technol.*, vol. 72, no. 7, pp. 8510–8525, Jul. 2023, doi: 10.1109/TVT.2023.3250957.

[36] C. Yu, Y. Feng, H. X. Liu, W. Ma, and X. Yang, "Corridor level cooperative trajectory optimization with connected and automated vehicles," *Transp. Res. C, Emerg. Technol.*, vol. 105, pp. 405–421, Aug. 2019, doi: 10.1016/j.trc.2019.06.002.

[37] D. Rey and M. W. Levin, "Blue phase: Optimal network traffic control for legacy and autonomous vehicles," *Transp. Res. B, Methodol.*, vol. 130, pp. 105–129, Dec. 2019, doi: 10.1016/j.trb.2019.11.001.

[38] Y. Zhang and C. G. Cassandras, "Decentralized optimal control of connected automated vehicles at signal-free intersections including comfort-constrained turns and safety guarantees," *Automatica*, vol. 109, Nov. 2019, Art. no. 108563, doi: 10.1016/j.automatica.2019.108563.

[39] R. Fourer, D. M. Gay, and B. W. Kernighan, "A modeling language for mathematical programming," *Manag. Sci.*, vol. 36, no. 5, pp. 519–554, May 1990.

[40] M. Choi, A. Rubenecia, and H. H. Choi, "Reservation-based traffic management for autonomous intersection crossing," *Int. J. Distrib. Sensor Netw.*, vol. 15, no. 12, Dec. 2019, Art. no. 155014771989595, doi: 10.1177/1550147719895956.

[41] A. Singh, M. S. Obaidat, S. Singh, A. Aggarwal, K. Kaur, B. Sadoun, M. Kumar, and K.-F. Hsiao, "A simulation model to reduce the fuel consumption through efficient road traffic modelling," *Simul. Model. Pract. Theory*, vol. 121, Dec. 2022, Art. no. 102658, doi: 10.1016/j.simpat.2022.102658.

[42] A. Zhou, S. Peeta, M. Yang, and J. Wang, "Cooperative signal-free intersection control using virtual platooning and traffic flow regulation," *Transp. Res. C, Emerg. Technol.*, vol. 138, May 2022, Art. no. 103610, doi: 10.1016/j.trc.2022.103610.

[43] R. Chen, J. Hu, M. W. Levin, and D. Rey, "Stability-based analysis of autonomous intersection management with pedestrians," *Transp. Res. C, Emerg. Technol.*, vol. 114, pp. 463–483, May 2020, doi: 10.1016/j.trc.2020.01.016.

[44] J. Sun, Z. Ma, T. Li, and D. Niu, "Development and application of an integrated traffic simulation and multi-driving simulators," *Simul. Model. Pract. Theory*, vol. 59, pp. 1–17, Dec. 2015, doi: 10.1016/j.simpat.2015.08.003.

[45] M. Mukadam, J. Dong, X. Yan, F. Dellaert, and B. Boots, "Continuous-time Gaussian process motion planning via probabilistic inference," *Int. J. Robot. Res.*, vol. 37, no. 11, pp. 1319–1340, Sep. 2018, doi: 10.1177/0278364918790369.

YANG LIU received the master's degree from the Changsha University of Science and Technology, in 2020, where he is currently pursuing the Ph.D. degree. His research interests include traffic control and intersection management.

KEJUN LONG received the B.S. degree from the Changsha University of Science and Technology, in 1996, and the Ph.D. degree from Tongji University, in 2005. From 2006 to 2011, he was an Associate Professor with the Changsha University of Science and Technology, where he has been a Professor, since 2011. He is currently the Dean of the Hunan Key Laboratory of Smart Roadway and Cooperative Vehicle-Infrastructure Systems, Changsha University of Science and Technology. His research interests include traffic control, traffic information technology, and intelligent transportation systems.

WEI WU received the Ph.D. degree from Tongji University, in 2013. He is currently a Professor with Chongqing Jiaotong University. His primary research interest includes traffic control and management within connected and autonomous vehicle environments.